

Expression and regulation of 1-acyl-*sn*-glycerol-3-phosphate acyltransferases in the epidermis

Biao Lu, Yan J. Jiang, Mao Q. Man, Barbara Brown, Peter M. Elias, and Kenneth R. Feingold¹

Dermatology and Medicine Services, Veterans Administration Medical Center and University of California School of Medicine, San Francisco, CA 94121

Abstract Phospholipids are a major class of lipids in epidermis, where they serve as a source of free fatty acids that are important for the maintenance of epidermal permeability barrier function. The phospholipid biosynthetic enzyme, 1-acyl-*sn*-glycerol-3-phosphate acyltransferase (AGPAT), catalyzes the acylation of lysophosphatidic acid to form phosphatidic acid, the major precursor of all glycerolipids. We identified an expression pattern of AGPAT isoforms that is unique to epidermis, with relatively high constitutive expression of mouse AGPAT (mAGPAT) 3, 4, and 5 but low constitutive expression of mAGPAT 1 and 2. Localization studies indicate that all five isoforms of AGPAT were expressed in all nucleated layers of epidermis. Furthermore, rat AGPAT 2 and 5 mRNAs increased in parallel with both an increase in enzyme activity and permeability barrier formation late in rat epidermal development. Moreover, after two methods of acute permeability barrier disruption, mAGPAT 1, 2, and 3 mRNA levels increased rapidly and were sustained for at least 24 h. In parallel with the increase in mRNA levels, an increase in AGPAT activity also occurred. Because upregulation of mAGPAT mRNAs after tape-stripping could be partially reversed by artificial barrier restoration by occlusion, these studies suggest that an increase in the expression of AGPATs is linked to barrier requirements.—Lu, B., Y. J. Jiang, M. Q. Man, B. Brown, P. M. Elias, and K. R. Feingold. Expression and regulation of 1-acyl-*sn*-glycerol-3-phosphate acyltransferases in the epidermis. *J. Lipid Res.* 2005. 46: 2448–2457.

Supplementary key words lamellar body • phospholipids • epidermal permeability barrier

The principal function of the epidermis is to provide a protective barrier against transcutaneous water loss (1, 2). This permeability barrier is localized to the stratum corneum, where three key lipids, cholesterol and ceramides as well as free fatty acids, form the extracellular lamellar membrane structures that mediate permeability barrier function (3, 4). In mammals, these lipid-enriched extracellular lamellar membranes derive from the exocytosis of lamellar bodies from the outmost stratum granulosum cells (1,

2). To form lamellar bodies, three precursor lipids, phospholipids along with cholesterol and glucosylceramides, are synthesized within the stratum spinosum and stratum granulosum cells (1, 2). After lamellar body secretion, phospholipids are further hydrolyzed in the extracellular domains of the stratum corneum to release hydrophobic essential and nonessential fatty acids that are required for the formation of a competent permeability barrier (5). Although phospholipids appear to be essential for epidermal permeability barrier function, little is known about their synthesis in normal epidermis or about the regulation of the enzymes of phospholipid synthesis.

1-Acyl-*sn*-glycerol-3-phosphate acyltransferase (AGPAT; EC 2.3.1.51), also known as lysophosphatidic acid acyltransferase, is the key enzyme of phospholipid and triglyceride biosynthesis. Several lines of evidence suggest that AGPAT should play a key role in the synthesis of phospholipids/triglycerides required for permeability barrier homeostasis. First, AGPAT catalyzes the further acylation of lysophospholipids to phosphatidic acid, the major precursor of all phospholipids/triglycerides. Second, some AGPAT isoforms are endoplasmic reticulum transmembrane proteins, so these enzyme isoforms would be situated at the correct location to produce phospholipids for lamellar body formation (6, 7). Third, AGPAT functions as an acyltransferase that transfers an acyl moiety onto the *sn*-2 position of the glycerol backbone. In most tissues, this position is largely occupied by a high prevalence of unsaturated fatty acids. Although the unsaturated, essential free fatty acid linoleic acid has been shown to be necessary for normal permeability barrier formation (8, 9), there is evidence that phospholipid-derived nonessential free fatty acids are also required for the barrier (5, 10). Finally, triglycerides, although not packaged in membrane in lamellar bodies, provide *N*-acyl fatty acids to sphingolipids, the most abundant barrier lipids (11, 12). Because of its apparent importance, a tight control of this acylation reaction is expected under normal physiological conditions.

Manuscript received 20 June 2005 and in revised form 28 July 2005.

Published, JLR Papers in Press, September 8, 2005.

DOI 10.1194/jlr.M500258.JLR200

¹ To whom correspondence should be addressed.
e-mail: kfeingold@itsa.ucsf.edu

Copyright © 2005 by the American Society for Biochemistry and Molecular Biology, Inc.

This article is available online at <http://www.jlr.org>

In mammals, multiple AGPAT isoforms have been identified (five in mice and six in humans), each encoded by a distinct gene (13–16). These isoforms display tissue-specific variation in expression and activity as well as different substrate preferences (7, 13, 15–17), which suggests tissue-specific functions (7, 17, 18). However, the biological significance of the existence of these variations in isoform expression remains largely unknown. Understanding the expression profile of these enzymes in epidermis, where there is a tissue-specific requirement for phospholipid synthesis for the barrier, could increase our understanding of how AGPAT participates in permeability barrier homeostasis and perhaps other epidermal functions. The aims of the present study are as follows: 1) to determine which AGPAT isoforms are expressed in the epidermis and their localization; 2) to determine the regulation of each isoform during fetal epidermal barrier development; and 3) to assess the regulation of isoform expression in relation to epidermal permeability barrier homeostasis.

MATERIALS AND METHODS

Materials

Female hairless mice (hl/hl), 8–12 weeks old, and timed pregnant Sprague-Dawley rats (plug date = day 0) were purchased from Simonsen Laboratories (Gilroy, CA). Acetone was purchased from Fisher Scientific (Fairlane, NJ). 5,5'-Dithiobis(2-nitrobenzoic acid), oleoyl- α -lysophosphatidic acid, and oleoyl CoA were purchased from Sigma (St. Louis, MO).

Experimental protocols

Epidermal barrier was disrupted by either tape-stripping or acetone treatment, as described previously (19–22). Impaired barrier function was monitored before and immediately after disruption by measurement of transepidermal water loss using an electrolytic water analyzer (MEECO, Warrington, PA). In some experiments, animals were occluded with a tightly fitted water vapor-impermeable latex membrane to artificially restore barrier function (20, 21, 23). To prepare epidermis from hairless mouse, flank skin was excised and epidermis was separated from dermis by incubating in 10 mM EDTA in Ca^{2+} - and Mg^{2+} -free phosphate-buffered saline (pH 7.4) at 37°C for 45 min. In another group of mice, the full-thickness skin was incubated in 10 mM DTT in PBS for 40 min at 37°C, and epidermal fractions (lower and upper layers) were prepared (24, 25). The separation occurs above the basal layer; thus, the lower layer comprises stratum basale and the upper layer comprises stratum granulosum, stratum spinosum, and stratum corneum. Epidermal samples were snap-frozen in liquid nitrogen and stored at -80°C until total RNA and protein extraction. The preparation of fetal rat epidermis was described previously (26, 27). Briefly, full-thickness skin was removed from fetus, and fetal epidermis was prepared using the protocol described above but with a shorter incubation time (30–35 min).

Isolation of total RNA and semiquantitative PCR

Total RNA was extracted from murine tissues and epidermis using TRIzol reagent according to the manufacturer's protocol (Invitrogen). The purity and the yield of isolated RNA were determined by monitoring the absorbance at optical densities of 260 and 280 nm. The integrity of the RNA was confirmed by performing denaturing gel electrophoresis on the isolated RNA samples. An aliquot of 1 μg of total RNA was reverse-transcribed with

20 ng of random hexamer (RT-for-PCR kit; Clontech, San Diego, CA) at 42°C for 1 h. The cDNA for each mouse AGPAT (mAGPAT) 1, 2, 3, 4, and 5 was amplified with a pair of specific primers. The primers were designed using Vector NTI Suite software for InforMax (version 7; Oxford, UK). For comparison purposes, all primer sets designed are located in different exons to avoid amplifying genomic DNA, and homologous full-length coding regions are amplified. The primer sets designed for mouse are also homologous to those of rats. All primers were synthesized by Qiagen (Alameda, CA). Each pair of primers, the primer sites, the lengths of predicted PCR products, and the GenBank accession number for each primer were reported previously (7). Primer sequences are as follows: mAGPAT 1, 5'-ACC AGA ATG GAG CTG TGG CC-3' (upper), 5'-CGC TCC CCC AGG CTT CTT CA-3' (lower); mAGPAT 2, 5'-CGC CGT CGG GGC TGG GGT GC-3' (upper), 5'-CTG GGC TGG CAA GAC CCC AG-3' (lower); mAGPAT 3, 5'-TGT TCT CAG TGA AGG ACC GT-3' (upper), 5'-CTT AAG CTC TTG GTT GCC AT-3' (lower); mAGPAT 4, 5'-GAT TTA TCT CTT GAG AAT CCC CAC ACC-3' (upper), 5'-GTC CGT TTG TTT CCG TTT GTT GTC-3' (lower); mAGPAT 5, 5'-AGA GGA TGC TGC TGT CCC T-3' (upper), 5'-AAC AAA CCA CAG GCA GCC-3' (lower); mAGPAT, 5'-TCC CCG TCT TCA GTA CCT TG-3' (upper), 5'-AAA ATG GCT GTG CAA AAT CC-3' (lower); internal control 36B4, 5'-GCG ACC TGG AAG TCC AAC TAC-3' (upper), 5'-ATC TGC TGC ATC TGC TTG G-3' (lower). All PCRs were carried out using an Eppendorf Mastercycler (96-well model). The validation of the quantitative measurement for each mAGPAT mRNA by RT-PCR was established previously (7). To ensure that the semiquantitative nature of the RT-PCR was valid using cDNA from skin epidermis, we performed the validation experiments using cDNA from mouse epidermis and confirmed that the method was accurate and reproducible. Briefly, under the RT-PCR conditions used, the levels of the PCR products were dependent on the amount of templates used in the reaction. At least an ~ 8 - to 10-fold difference of cDNA concentration of each mAGPAT was detected.

Preparation of whole cell extracts and AGPAT enzyme activity assay

Whole cell extracts were prepared by a brief 30 s homogenization (Kinematica, Kriens-Luzern, Switzerland) followed by three rounds of sonification (10 s/round) on ice with the Sonifier (Cell Disruptor 350; Branson Sonic Power Co.) in a buffer containing 100 mM Tris-HCl (pH 7.4), 3 mM MgCl_2 , and 1 unit of proteinase inhibitors (proteinase inhibitor cocktail; Sigma). Subsequently, the cell lysate was centrifuged at 3,000 rpm for 10 min to remove cell debris, and the resulting supernatant was saved for protein and enzyme assay. The protein concentration of whole cell extract was determined by Bio-Rad Protein Assay (Bio-Rad Laboratories, Inc., Hercules, CA) using BSA as a standard. AGPAT enzyme activity was determined spectrophotometrically using 50 μM oleoylglycerol-phosphate and 40 μM oleoyl-CoA as described (28, 29).

Statistical analysis

The results are expressed as means \pm SEM. Statistical significance between two experimental groups was determined using Student's *t*-test. A value of $P < 0.05$ was considered significant.

RESULTS

Epidermis displays a unique AGPAT expression profile

In murine tissues, AGPAT exists in at least five isoforms. Our initial studies have focused on determining the pattern and relative expression levels of AGPAT isoforms in murine epidermis. To compare the relative abundance of

each isoform, similar sets of primers were designed and the same epidermal cDNAs were used for all isoform amplification. The specific amplification and semiquantitative measurement for each mAGPAT mRNA have been established (7) and confirmed in this study using cDNA from mouse epidermis (data not shown). As shown in **Fig. 1A**, the expression pattern of mAGPATs in epidermis was unique. Both mAGPAT 1 and 2 mRNAs were low in murine epidermis, compared with the high expression levels of these isoforms in other tissues, including brain, heart, lung, liver, kidney, and spleen. In contrast, relatively high levels of expression for mAGPAT 3, 4, and 5 were observed in the epidermis compared with other tissues (**Fig. 1A**). These studies show that the expression profile of mAGPAT isoforms differs in epidermis compared with other murine tissues.

For a more detailed analysis, we next compared epidermal AGPAT expression with isoform patterns in extracutaneous mouse organs, including lung, liver, and kidney, that exhibit particularly high rates of lipid metabolism. As shown in **Fig. 1B**, the epidermal expression of mAGPAT 1 was ~9% of that in lung ($P < 0.001$), ~27% of that in liver ($P < 0.05$), and ~6% of that in kidney ($P < 0.001$). The levels of mAGPAT 2 mRNA were also lower in epidermis: ~10.8% of that in lung ($P < 0.001$), ~1% of that in liver ($P < 0.001$), and ~3% of that in kidney ($P < 0.001$). However, moderate levels of mAGPAT 3 were observed in epidermis (~20–35%) compared with lung, liver, and kidney levels. Strikingly, mAGPAT 5 was the only isoform that exhibited a higher level of constitutive expression in epidermis relative to the other tissues analyzed: ~2-fold higher than in lung and liver ($P < 0.001$) and 60–70% greater than in kidney ($P < 0.001$). Together, these studies indicate a unique pattern of expression of mAGPATs in murine epidermis, which also differs greatly from other tissue with high rates of lipid synthesis.

Epidermal AGPAT isoforms are expressed in all nucleated layers

The epidermis generates a broad range of lipid species (30, 31). Although significant amounts of lipids are synthesized in the basal layer, lipid synthesis continues in all of the nucleated layers of the epidermis (32). To determine the localization of mAGPAT isoforms, we next measured mAGPAT mRNA levels in the lower versus upper layers of epidermis. Using the DTT method (24, 25), we separated fractions of lower (stratum basale) and upper (stratum spinosum, stratum granulosum, and stratum corneum) epidermis. To obtain sufficient signals for mAGPAT 1 and 2, PCR conditions were optimized and 32 cycles, instead of 25, were used for PCR amplification. As shown in **Fig. 2A**, mAGPAT 1 and 2 exhibited higher expression levels in the lower than in the upper epidermis. However, there was no significant difference in mAGPAT 1 and 2 mRNA levels in lower versus upper epidermis when the results were normalized to an internal control (i.e., 36B4) (**Fig. 2B**). Furthermore, AGPAT 3, 4, and 5 also displayed no differences in mRNA levels in lower versus upper epidermis. These results show that AGPAT mRNAs are expressed throughout the nucleated layers of murine epidermis.

A subset of rat AGPAT isoforms increase in parallel with fetal skin barrier development

To begin to ascertain the functions of AGPAT in epidermis, we next assessed isoform expression in fetal epidermis, where barrier function is established during the last trimester (33, 34). During this period, the epidermis stratifies and most of the enzymes required for permeability barrier lipid synthesis begin to be expressed at high levels (26, 27, 35). In the fetal rat, epidermal stratification begins on day 17, a burst of lipid synthesis occurs on day 19,

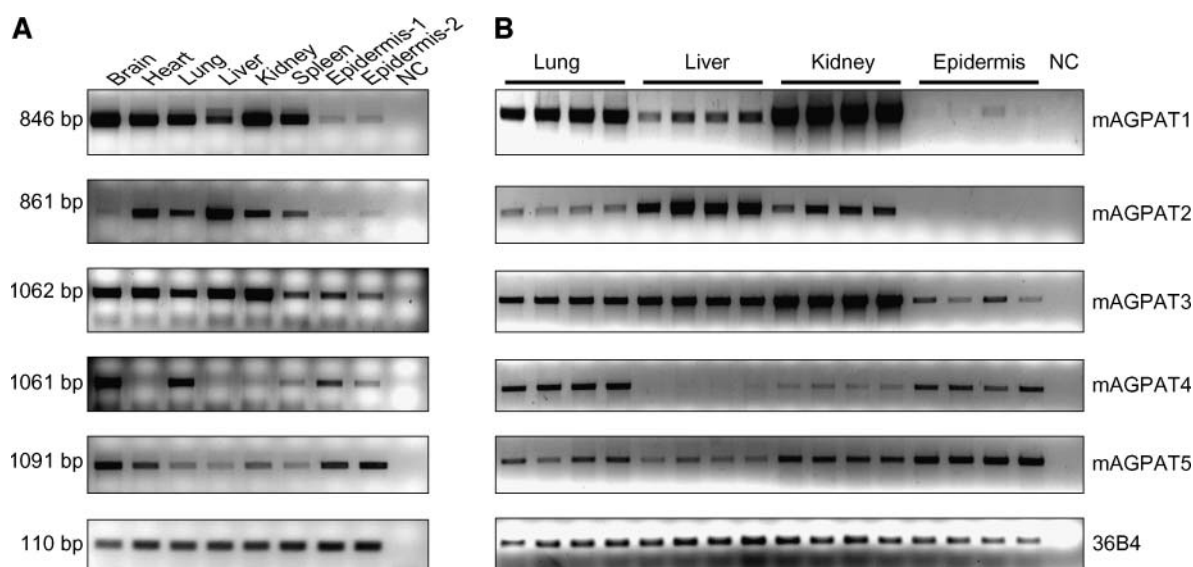


Fig. 1. mRNA expression profile of mouse 1-acyl-*sn*-glycerol-3-phosphate acyltransferase (mAGPAT) isoforms in murine tissues. Mouse organ and epidermal samples were prepared. Total RNA was extracted and RT-PCR was performed as described in Materials and Methods. A: Representative gel image of PCR products of each mouse AGPAT (mAGPAT) isoform and the internal control 36B4 gene. NC, negative control. B: Representative gel image of PCR products of each mAGPAT isoform from several selected tissues ($n = 4$).

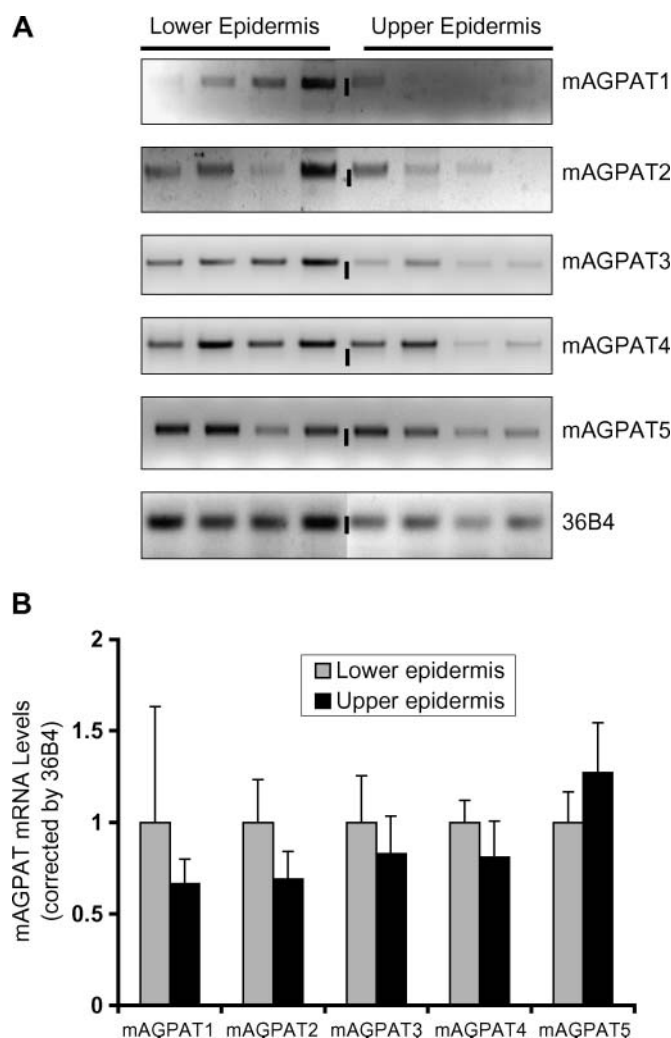


Fig. 2. mAGPAT expression in the lower and upper layers of murine epidermis. The lower and upper layers of epidermis were prepared as described in Materials and Methods. Total RNA was extracted and RT-PCR was performed. A: Representative gel image of PCR products for each isoform and the internal control 36B4. B: Densitometry values normalized with 36B4 for each mAGPAT isoform. Data are presented as means \pm SEM ($n = 4$).

a multilayered stratum corneum with a competent barrier to water loss is formed between days 19 and 21, and pups are born with a competent barrier on day 22 (36). To determine the potential regulation of rat AGPATs (rAGPATs) during fetal barrier ontogenesis, epidermis was collected from pups over this time period (days 17, 18, 19, 21, and 22) and both rAGPAT mRNA levels and total AGPAT activity were determined. As shown in **Fig. 3**, the mRNA levels for both rAGPAT 2 and 5 increased progressively, peaking on day 19, whereas the mRNA levels for rAGPAT 1, 3, and 4 remained unchanged. In contrast, all AGPAT isoforms and several housekeeping controls, including 36B4, 18S rRNA, and GAPDH (data not shown), declined late in late gestation (i.e., days 21 and 22). Together, these data show that a subset of rAGPAT isoforms (isoforms 2 and 5) increase during fetal skin development, but this upregulation was specific, because other rAGPAT isoforms were not modulated similarly during late gestation. We next

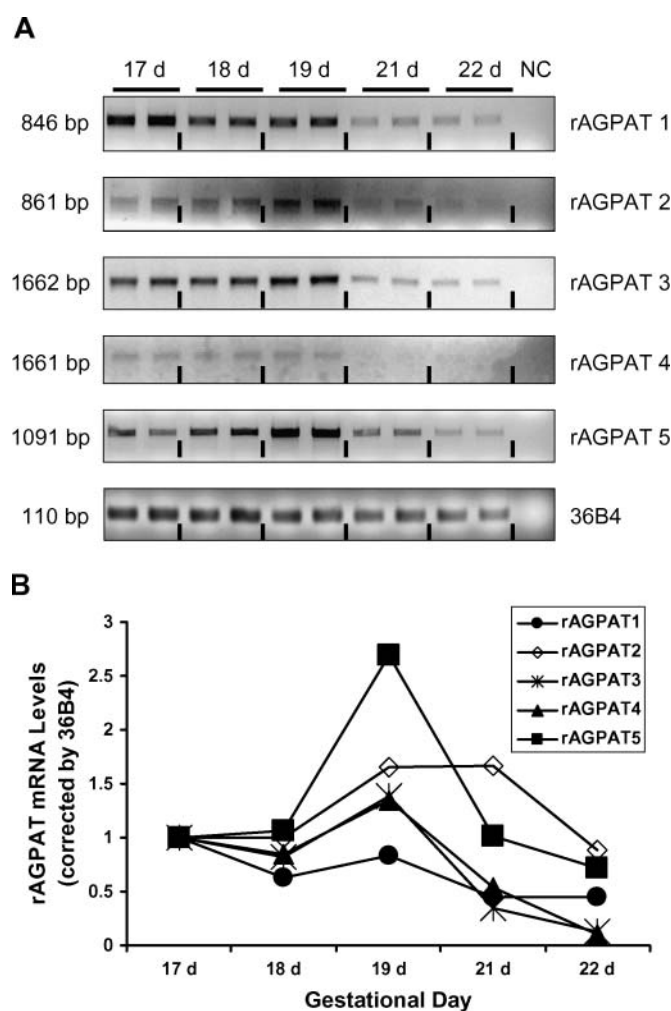


Fig. 3. Rat AGPAT (rAGPAT) expression during fetal skin barrier development. Rat fetal epidermis was prepared as described in Materials and Methods. Total RNA was extracted and RT-PCR was performed. A: Representative gel image of PCR products for each rAGPAT isoform and the internal control 36B4. NC, negative control. B: Densitometry values normalized with 36B4 for each isoform. Data are presented as means \pm SEM ($n = 2$). Note that day 17 and 18 samples were pooled from three to five fetal epidermises.

measured total enzyme activity of AGPAT, which assesses the net contribution of all AGPAT isoforms in fetal epidermal tissue lysates. As shown in **Fig. 4**, an increase in AGPAT activity occurs on day 19 (1.156 nmol/ μ g/min) versus day 17 (0.796 nmol/ μ g/min). Although the rAGPAT mRNA levels largely decreased on day 21 compared with levels on days 17 and 19, AGPAT activity remained relatively high (1.034 nmol/ μ g/min) on day 21. Thus, the increase in rAGPAT transcripts described above may contribute to the increase in total AGPAT activity. Together, these results suggest that phospholipid/triglyceride biosynthesis increases late in fetal development, in parallel with barrier formation.

Permeability barrier disruption upregulates selected mAGPAT isoforms

To determine the potential role of these AGPAT isoforms in maintaining permeability barrier homeostasis, we next

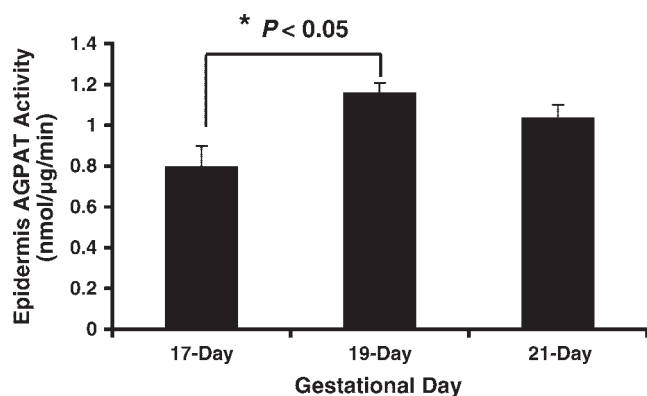


Fig. 4. AGPAT activity in fetal rat epidermis. Rat fetal skin epidermis was prepared as described in Materials and Methods. AGPAT enzyme activities were determined using epidermal extracts from day 17, 19, and 21 samples. Data are presented as means \pm SEM ($n = 3$). Note that day 17 and 18 samples were pooled from three to five fetal skin epidermises.

assessed the effects of acute barrier disruption on mAGPAT isoform expression profiles. Under our experimental conditions, a >50 -fold increase in transepidermal water loss was obtained using either tape-stripping or acetone application to achieve acute barrier disruption (5). In the tape-stripping model, we next monitored changes in mAGPAT mRNA levels over time. Tape-stripping resulted in a rapid increase in the mRNA levels of mAGPAT 1, 2, and 3, a change that was detected as early as 1 h after acute disruption and that was sustained for at least 24 h (Fig. 5A, B). In contrast, the mRNA level of mAGPAT 4 did not change, whereas mAGPAT5 increased minimally at 1 h followed by small decreases at 3 and 6 h, returning to baseline at 24 h (Fig. 5). To further verify these observations, we next determined whether a comparable pattern of upregulation of epidermal mAGPAT mRNA levels occurs after the acetone-induced barrier disruption. Because isoform expression changed most at 1 h after tape-stripping, we chose this time point for our studies with acetone. As shown in Fig. 6A, B, mAGPAT 1, 2, 3, and 5 levels increased rapidly, whereas mAGPAT 4 mRNA levels did not change with tape-stripping. Finally, we assessed barrier-induced changes in mRNA levels of each isoform in the lower versus upper epidermis. As shown in Fig. 7, a slight but statistically significant increase in mAGPAT 5 mRNA occurred in upper versus lower epidermis after tape-stripping ($\sim 16\%$; $P < 0.05$), whereas slightly less mAGPAT 3 mRNA was expressed in the upper versus lower epidermis ($\sim 18\%$; $P < 0.05$). Thus, disruption of the epidermal permeability barrier stimulates an increase in the mRNA levels of a subset of mAGPATs, independent of the method of barrier disruption used.

Previous studies have shown that a number of the enzymes responsible for epidermal lipid biosynthesis are upregulated after barrier disruption and that this upregulation can be blocked by artificial barrier restoration (11, 37). Therefore, we next determined whether the previously observed increase in the expression of mAGPATs could be blocked by occlusion with a vapor-impermeable membrane

that artificially normalizes barrier function. As shown in Fig. 8A, B, the expected upregulation of mAGPAT 1, 2, and 3 after tape-stripping could be partially reversed if an occlusive membrane was placed immediately after acute barrier disruption.

Finally, we assessed whether the increase in AGPAT expression after barrier disruption produced a parallel increase in enzyme activity. As shown in Fig. 9, tape-stripping produced a 26% increase in total AGPAT activity (tape = $1.429 \text{ nmol}/\mu\text{g}/\text{min}$ versus control = $1.135 \text{ nmol}/\mu\text{g}/\text{min}$; $P < 0.05$). Together, these studies indicate that specific mAGPAT isoforms are regulated specifically by permeability barrier requirements, leading to increased enzyme activity, further evidence for the potential role of AGPAT in maintaining permeability barrier homeostasis.

Permeability barrier disruption does not alter the expression of mitochondrial *sn*-glycerol-3-phosphate acyltransferase

Because a subset of microsomal AGPATs were upregulated in responding to permeability barrier requirements, we next assessed whether mitochondrial *sn*-glycerol-3-phosphate acyltransferase (GPAT) was also similarly upregulated after barrier disruption. As shown in Fig. 10, mitochondrial GPAT expression did not change at the 3 h time point after tape-stripping. Thus, the microsomal acyltransferases, but not mitochondrial acyltransferases, are modulated after barrier disruption.

DISCUSSION

The formation of the stratum corneum in the epidermis requires active de novo synthesis of phospholipids. Much of the newly synthesized phospholipids together with glycosphingolipid and cholesterol are initially assembled into lamellar bodies and subsequently secreted into the interstices of stratum corneum, where they mediate permeability barrier function (1, 2, 4). Given the critical role of phospholipids in permeability barrier maintenance, it is important to determine the pathways of phospholipid biosynthesis and their regulation in epidermis. In the present study, we demonstrate for the first time a unique pattern of expression of AGPAT isoforms in murine epidermis. In addition, we show that certain of these AGPAT isoforms increase both during fetal permeability barrier development and after acute barrier disruption. These findings indicate that an increase in AGPAT-mediated phospholipid synthesis could play a critical role in both normal skin permeability barrier homeostasis and during formation of the barrier in utero.

The stratum corneum lipid mixture that mediates permeability barrier function originates from the exocytosis of lamellar bodies. Lamellar bodies are specialized membrane-bound secretory organelles that contain abundant phospholipids. To provide sufficient substrates for phospholipid synthesis, keratinocytes first must synthesize non-essential fatty acids as well as take up essential fatty acids

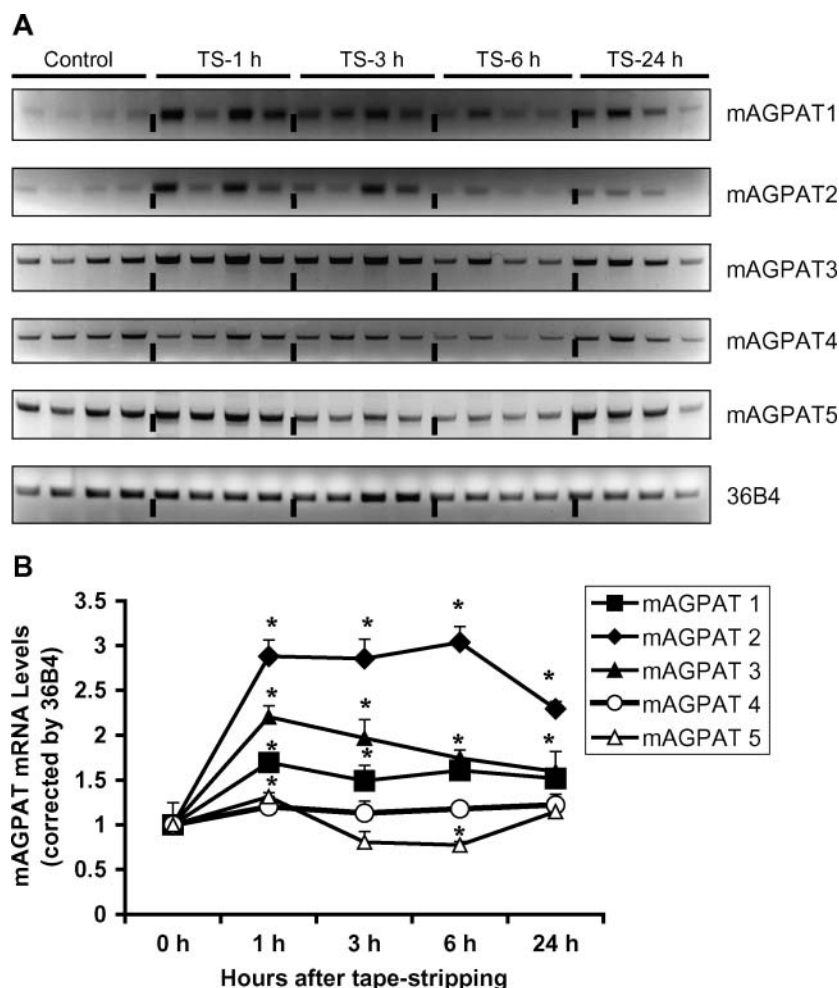


Fig. 5. Time course of mAGPAT expression in murine epidermis after acute barrier disruption. Mouse skin was tape-stripped or unstripped (for each side of the back skin from the same mouse; the unstripped side serves as a control) as described in Materials and Methods. Skin samples were collected at the indicated time points, and epidermis was prepared. Total RNA was extracted and RT-PCR was performed. A: Representative gel image of PCR products for each mAGPAT isoform and 36B4. B: Densitometry values normalized with 36B4 for each isoform. Data are presented as means \pm SEM ($n = 4$). * $P < 0.05$.

from the circulation (8–10). Epidermis is thus a highly active lipid synthetic tissue, which generates abundant free fatty acids destined not only for barrier but also for membrane biogenesis. Because of the potential detergent action of free fatty acids, the intracellular fatty acids are quickly assembled into complex, nontoxic species, such as phospholipids and triglycerides, by the action of phospholipid acyltransferases.

In mammalian cells, two major phospholipid acyltransferases catalyze glycerolipid biosynthesis (i.e., GPAT and AGPAT). GPAT mediates the acylation of glycerol-3-phosphate at the *sn*-1 position, which is the first committed step in glycerolipid biosynthesis, whereas AGPAT mediates the second acylation reaction by catalyzing the transfer of another acyl chain to the *sn*-2 position on the glycerol backbone (38, 39). Both GPAT and AGPAT have multiple enzyme isoforms, which localize to endoplasmic reticulum and mitochondrial membranes (6, 40, 41). Lamellar body lipids are derived mainly from endoplasmic reticulum; thus, microsomal GPAT/AGPAT isoforms are more im-

portant for lamellar body formation. Because microsomal GPAT has not yet been cloned, studies on the regulation of microsomal GPAT are not yet possible. However, mitochondrial GPAT has been cloned, and its expression did not change after barrier disruption (Fig. 10). Thus, the microsomal acyltransferases, but not mitochondrial acyltransferases, are likely modulated after barrier disruption.

One of the major aims of the present study was to determine the pattern of expression and the localization of AGPAT isoforms in murine epidermis. Although a high mRNA level of mAGPAT 1 has been demonstrated in most organs analyzed (brain, heart, lung, liver, and kidney), very low levels of constitutive expression were detected in murine epidermis. Similarly, mAGPAT 2 exhibited high basal levels of expression in most other organs, but its constitutive expression was low in epidermis. Consistent with previous observations that the level of AGPAT 3 is variably expressed in extracutaneous organs (7), its expression in epidermis was moderate. Interestingly, AGPAT 4 exhibited a relatively high constitutive expression in epi-

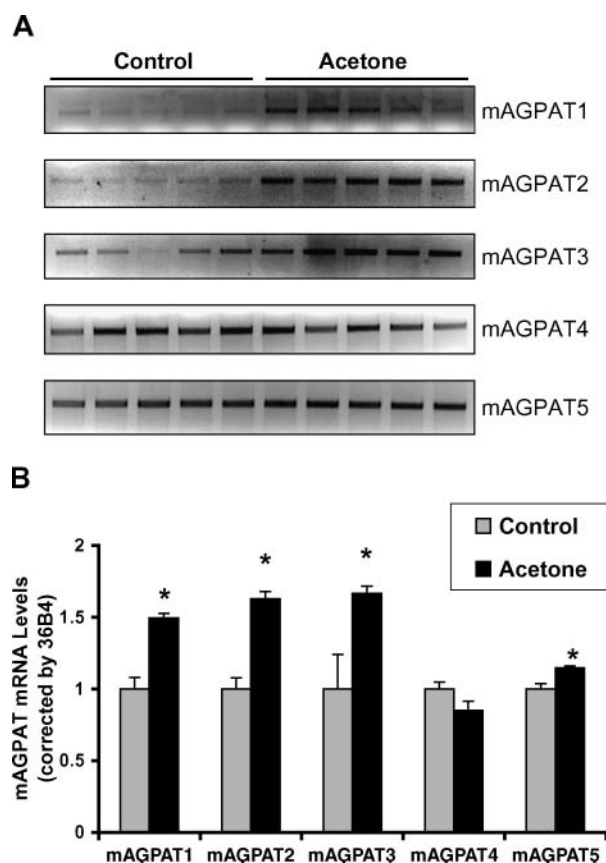


Fig. 6. mAGPAT expression in murine epidermis after acetone application. Mouse skin was treated with acetone or PBS (for each side of the back skin from the same mouse; the PBS side serves as a control) as described in Materials and Methods. After 1 h, skin samples were collected and epidermis was prepared. Total RNA was then extracted and RT-PCR was performed. A: Representative gel image of PCR products for each isoform and 36B4. B: Densitometry values normalized with 36B4 for each isoform. Data are presented as means \pm SEM ($n = 5$). * $P < 0.05$.

dermis, as this isoform was barely detectable in several other organs, such as heart, liver, kidney, and spleen, and AGPAT 5 had the highest constitutive expression compared with those of other isoforms. To further define the localization of AGPAT isoforms in different layers of epidermis, we examined the mRNA levels of AGPAT isoforms in the lower and upper layers of epidermis. Under basal conditions, no significant difference was found for any of those isoforms in the lower versus upper layers of epidermis, suggesting that phospholipid biosynthesis may be a continuous process that occurs in all of the nucleated layers of epidermis. The data demonstrated low constitutive expression for mAGPAT isoforms 1 and 2 but high constitutive expression for mAGPAT isoforms 3, 4, and 5. This unique profile of AGPAT expression in epidermis indicates that a tissue-specific composition of these enzymes might be required for proper epidermal function.

Although multiple enzymes have been designated as AGPATs, the functional role of these isoforms has not yet been firmly established. According to sequence identities, these five isoforms can be further divided into three sub-

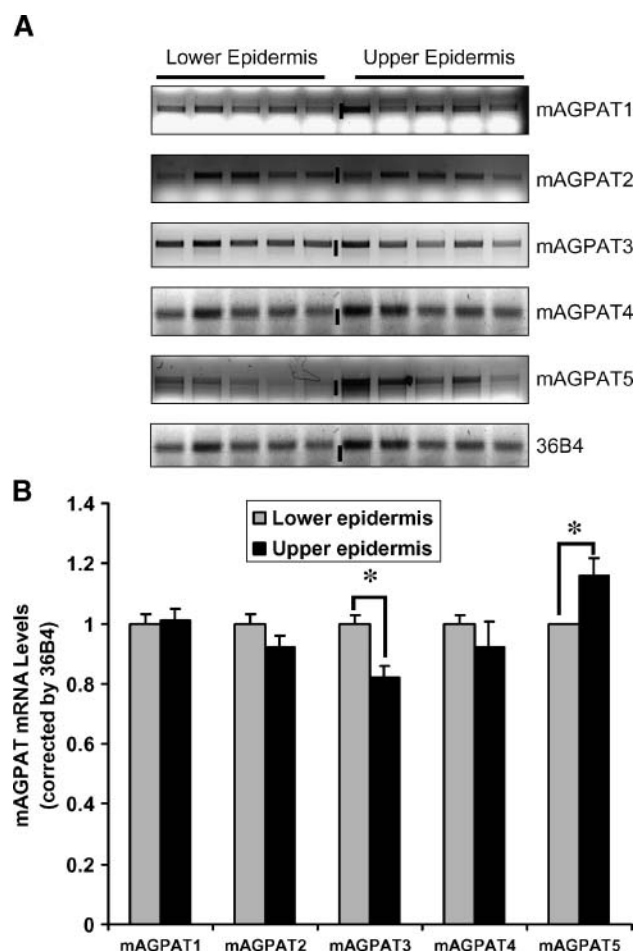


Fig. 7. mAGPAT expression in the lower and upper layers of epidermis after tape-stripping. Mouse skin was tape-stripped, and after 3 h the lower and upper layers of epidermis were prepared as described in Materials and Methods. Total RNA was extracted and RT-PCR was performed. A: Representative gel image of PCR products for each mAGPAT isoform and 36B4. B: Densitometry values normalized with 36B4 for each isoform. Data are presented as means \pm SEM ($n = 5$). * $P < 0.05$.

groups: group I (AGPAT 1 and 2); group II (AGPAT 3 and 4); and group III (AGPAT 5) (7). It appears that group I enzymes confer relatively higher acyltransferase activities than enzymes in either group II or group III (7). However, data from this study show that both group II and group III enzymes display high basal expression in adult murine epidermis. One possible explanation is that enzymes in groups II and III may be involved in maintaining basal barrier function when phospholipid synthesis is not subject to increased demand. In support of this notion, group I enzymes appear to be upregulated during fetal epidermal ontogenesis (AGPAT 2) and during barrier repair (AGPAT 1 and 2). In these conditions, AGPAT 1 and/or AGPAT 2 are upregulated in parallel with a burst of barrier lipid biosynthesis. Yet, the question remains why mammalian tissues express multiple isoforms of an enzyme that catalyzes the same biochemical reaction. Presumably, different enzyme isoforms could localize to discrete subcellular compartments, or they could exhibit different substrate

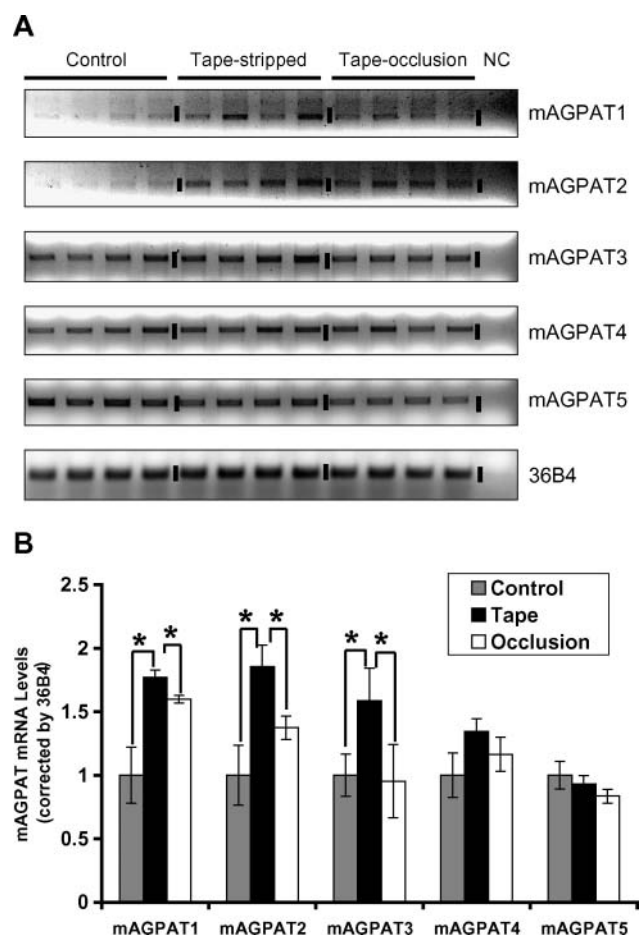


Fig. 8. mAGPAT expression in murine epidermis after tape-stripping. Mouse skin was tape-stripped, tape-stripped plus occlusion, or unstripped (for each side of the back skin from the same mouse; the unstripped side serves as a control) as described in Materials and Methods. After 3 h, epidermis was prepared. Total RNA was extracted and RT-PCR was performed. **A:** Representative gel image of PCR products for each mAGPAT isoform and 36B4. NC, negative control. **B:** Densitometry values normalized with 36B4 for each isoform. Data are presented as means \pm SEM ($n = 4$). * $P < 0.05$.

preferences (i.e., they could incorporate different fatty acid species into phospholipids). Finally, these isoforms could provide regulatory mechanisms in response to certain requirements, such as cell repair, growth, proliferation, and/or lipid synthesis (42, 43). These assumptions are supported by the fact that many other enzymes in lipid metabolism also exist as duplicate/multiple isoforms with discrete localization, function, and regulation (6, 43, 44).

Among AGPAT isoforms, the largest body of information is known for AGPAT 1 and 2. mAGPAT 1 shares 44% sequence identity with AGPAT 2 and much less homology with the three other isoforms (<11% sequence identity). Several studies have suggested that AGPAT 1 is expressed ubiquitously in most tissues and hence functions as a housekeeping gene (13, 14). In contrast, the expression of AGPAT 2 is more tissue-specific; it is expressed at high levels in liver, heart, and adipose tissue, at intermediate levels in kidney, lung, and spleen, at very low levels in epidermis, and is almost undetectable in brain. Linkage stud-

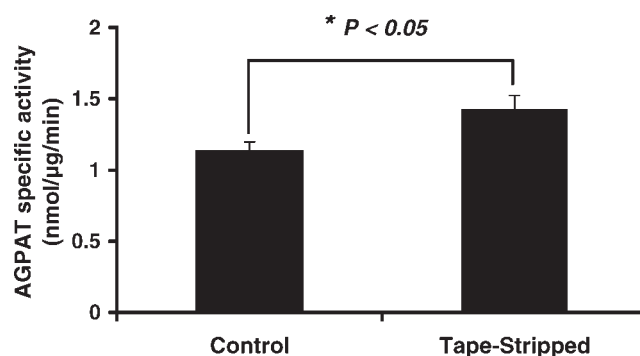


Fig. 9. mAGPAT enzyme activity in epidermis after tape-stripping. Mouse skin was tape-stripped or unstripped (for each side of the back skin from the same mouse; the unstripped side serves as a control), and epidermis was prepared after 3 h. Whole cell extracts from epidermis were prepared, and total AGPAT enzyme activities were assayed as described in Materials and Methods. Data are presented as means \pm SEM ($n = 5$). * $P < 0.05$.

ies have revealed that AGPAT 2 is critical for triglyceride biosynthesis (18). Mutations in human AGPAT 2 have been shown to be one of the causes of congenital generalized lipodystrophy by inhibiting triacylglycerol synthesis in adipocytes (18, 45). Of note, triglycerides are a major component of lipids in epidermis and constitute ~12% and ~24% of total weight in the basal/spinous and granular layers, respectively (38, 39). Recently, additional roles for AGPAT 2 have emerged. AGPAT 2, but not AGPAT 1, may play a role in providing proliferative/survival signals in normal and malignant cells, presumably by generating

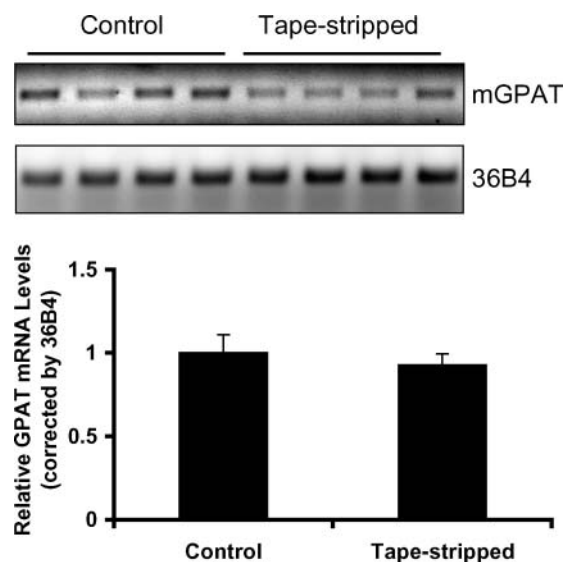



Fig. 10. Expression of mitochondrial *sn*-glycerol-3-phosphate acyltransferase (GPAT) in mouse epidermis before and after tape-stripping. Mouse skin was either tape-stripped or unstripped (for each side of the back skin from the same mouse; the unstripped side serves as a control) as described in Materials and Methods. After 3 h, skin samples were collected and epidermis was prepared. Total RNA was then extracted and RT-PCR was performed. Upper panel: Representative gel image of PCR products of mitochondrial GPAT and 36B4 obtained from RT-PCR. Lower panel: Densitometry values normalized with 36B4 for mitochondrial GPAT.

phosphatidic acid, an important intracellular secondary messenger (42, 46, 47). We speculate that AGPAT 2 might perform these two functions in skin epidermis. For example, AGPAT 2 has a low constitutive expression but is induced during fetal epidermal development or after epidermal barrier disruption (Figs. 3, 5). In these two situations, the upregulation of AGPAT 2 parallels a burst of both cell proliferation and barrier lipid synthesis.

In summary, we have identified a unique expression pattern of AGPAT isoforms in murine epidermis, with both constitutive (isoforms 3, 4, and 5) and/or inducible (isoforms 1, 2, 3, and 5) forms present. The temporal regulation of AGPATs during normal epidermal development and during barrier repair suggests that an increase in epidermal phospholipid synthesis may play a role in maintaining epidermal permeability barrier homeostasis. 

REFERENCES

- Elias, P. M., and K. R. Feingold. 1999. Skin as an organ of protection. In *Fitzpatrick's Dermatology in General Medicine*. I. Freedberg, et al., editors. McGraw-Hill, Philadelphia. 164–174.
- Elias, P. M., and K. R. Feingold. 1992. Lipids and the epidermal water barrier: metabolism, regulation, and pathophysiology. *Semin. Dermatol.* **11**: 176–182.
- Schurer, N. Y., and P. M. Elias. 1991. The biochemistry and function of stratum corneum lipids. *Adv. Lipid Res.* **24**: 27–56.
- Feingold, K. R. 1991. The regulation and role of epidermal lipid synthesis. *Adv. Lipid Res.* **24**: 57–82.
- Mao-Qiang, M., K. R. Feingold, M. Jain, and P. M. Elias. 1995. Extracellular processing of phospholipids is required for permeability barrier homeostasis. *J. Lipid Res.* **36**: 1925–1935.
- Coleman, R. A., and D. P. Lee. 2004. Enzymes of triacylglycerol synthesis and their regulation. *Prog. Lipid Res.* **43**: 134–176.
- Lu, B., Y. J. Jiang, Y. Zhou, F. Y. Xu, G. M. Hatch, and P. C. Choy. 2005. Cloning and characterization of murine 1-acyl-sn-glycerol 3-phosphate acyltransferases and their regulation by PPARalpha in murine heart. *Biochem. J.* **385**: 469–477.
- Elias, P. M., and B. E. Brown. 1978. The mammalian cutaneous permeability barrier: defective barrier function is essential fatty acid deficiency correlates with abnormal intercellular lipid deposition. *Lab. Invest.* **39**: 574–583.
- Elias, P. M., B. E. Brown, and V. A. Ziboh. 1980. The permeability barrier in essential fatty acid deficiency: evidence for a direct role for linoleic acid in barrier function. *J. Invest. Dermatol.* **74**: 230–233.
- Mao-Qiang, M., P. M. Elias, and K. R. Feingold. 1993. Fatty acids are required for epidermal permeability barrier function. *J. Clin. Invest.* **92**: 791–798.
- Holleran, W. M., K. R. Feingold, M. Q. Man, W. N. Gao, J. M. Lee, and P. M. Elias. 1991. Regulation of epidermal sphingolipid synthesis by permeability barrier function. *J. Lipid Res.* **32**: 1151–1158.
- Holleran, W. M., M. Q. Man, W. N. Gao, G. K. Menon, P. M. Elias, and K. R. Feingold. 1991. Sphingolipids are required for mammalian epidermal barrier function. Inhibition of sphingolipid synthesis delays barrier recovery after acute perturbation. *J. Clin. Invest.* **88**: 1338–1345.
- Eberhardt, C., P. W. Gray, and L. W. Tjoelker. 1997. Human lysophosphatidic acid acyltransferase. cDNA cloning, expression, and localization to chromosome 9q34.3. *J. Biol. Chem.* **272**: 20299–20305.
- Eberhardt, C., P. W. Gray, and L. W. Tjoelker. 1999. cDNA cloning, expression and chromosomal localization of two human lysophosphatidic acid acyltransferases. *Adv. Exp. Med. Biol.* **469**: 351–356.
- Stamps, A. C., M. A. Elmore, M. E. Hill, K. Kelly, A. A. Makda, and M. J. Finnen. 1997. A human cDNA sequence with homology to non-mammalian lysophosphatidic acid acyltransferases. *Biochem. J.* **326**: 455–461.
- West, J., C. K. Tompkins, N. Balantac, E. Nudelman, B. Meengs, T. White, S. Bursten, J. Coleman, A. Kumar, J. W. Singer, et al. 1997. Cloning and expression of two human lysophosphatidic acid acyltransferase cDNAs that enhance cytokine-induced signaling responses in cells. *DNA Cell Biol.* **16**: 691–701.
- Aguado, B., and R. D. Campbell. 1998. Characterization of a human lysophosphatidic acid acyltransferase that is encoded by a gene located in the class III region of the human major histocompatibility complex. *J. Biol. Chem.* **273**: 4096–4105.
- Agarwal, A. K., E. Arioglu, S. De Almeida, N. Akkoc, S. I. Taylor, A. M. Bowcock, R. I. Barnes, and A. Garg. 2002. AGPAT2 is mutated in congenital generalized lipodystrophy linked to chromosome 9q34. *Nat. Genet.* **31**: 21–23.
- Menon, G. K., K. R. Feingold, A. H. Moser, B. E. Brown, and P. M. Elias. 1985. De novo sterologenesis in the skin. II. Regulation by cutaneous barrier requirements. *J. Lipid Res.* **26**: 418–427.
- Grubauer, G., P. M. Elias, and K. R. Feingold. 1989. Transepidermal water loss: the signal for recovery of barrier structure and function. *J. Lipid Res.* **30**: 323–333.
- Grubauer, G., K. R. Feingold, and P. M. Elias. 1987. Relationship of epidermal lipogenesis to cutaneous barrier function. *J. Lipid Res.* **28**: 746–752.
- Proksch, E., K. R. Feingold, M. Q. Man, and P. M. Elias. 1991. Barrier function regulates epidermal DNA synthesis. *J. Clin. Invest.* **87**: 1668–1673.
- Feingold, K. R., B. E. Brown, S. R. Lear, A. H. Moser, and P. M. Elias. 1986. Effect of essential fatty acid deficiency on cutaneous sterol synthesis. *J. Invest. Dermatol.* **87**: 588–591.
- Feingold, K. R., B. E. Brown, S. R. Lear, A. H. Moser, and P. M. Elias. 1983. Localization of de novo sterologenesis in mammalian skin. *J. Invest. Dermatol.* **81**: 365–369.
- Proksch, E., P. M. Elias, and K. R. Feingold. 1991. Localization and regulation of epidermal 3-hydroxy-3-methylglutaryl-coenzyme A reductase activity by barrier requirements. *Biochim. Biophys. Acta.* **1083**: 71–79.
- Hanley, K., Y. Jiang, W. M. Holleran, P. M. Elias, M. L. Williams, and K. R. Feingold. 1997. Glucosylceramide metabolism is regulated during normal and hormonally stimulated epidermal barrier development in the rat. *J. Lipid Res.* **38**: 576–584.
- Hanley, K., Y. Jiang, C. Katagiri, K. R. Feingold, and M. L. Williams. 1997. Epidermal steroid sulfatase and cholesterol sulfotransferase are regulated during late gestation in the fetal rat. *J. Invest. Dermatol.* **108**: 871–875.
- Lands, W. E., and P. Hart. 1965. Metabolism of glycerolipids. VI. Specificities of acyl coenzyme A:phospholipid acyltransferases. *J. Biol. Chem.* **240**: 1905–1911.
- Yamashita, S., and S. Numa. 1981. Glycerophosphate acyltransferase from rat liver. *Methods Enzymol.* **71**: 550–554.
- Nicolaides, N. 1974. Skin lipids: their biochemical uniqueness. *Science.* **186**: 19–26.
- Feingold, K. R., M. H. Wiley, A. H. Moser, D. T. Lau, S. R. Lear, and M. D. Siperstein. 1982. De novo sterologenesis in intact primates. *J. Lab. Clin. Med.* **100**: 405–410.
- Monger, D. J., M. L. Williams, K. R. Feingold, B. E. Brown, and P. M. Elias. 1988. Localization of sites of lipid biosynthesis in mammalian epidermis. *J. Lipid Res.* **29**: 603–612.
- Cartledge, P., and N. Rutter. 1992. Skin barrier function. In *Fetal and Neonatal Physiology*. R. Polin and W. Fox, editors. W.B. Saunders, Philadelphia. 569–585.
- Hanley, K., U. Rassner, P. M. Elias, M. L. Williams, and K. R. Feingold. 1996. Epidermal barrier ontogenesis: maturation in serum-free media and acceleration by glucocorticoids and thyroid hormone but not selected growth factors. *J. Invest. Dermatol.* **106**: 404–411.
- Hanley, K., Y. Jiang, P. M. Elias, K. R. Feingold, and M. L. Williams. 1997. Acceleration of barrier ontogenesis in vitro through air exposure. *Pediatr. Res.* **41**: 293–299.
- Aszterbaum, M., G. K. Menon, K. R. Feingold, and M. L. Williams. 1992. Ontogeny of the epidermal barrier to water loss in the rat: correlation of function with stratum corneum structure and lipid content. *Pediatr. Res.* **31**: 308–317.
- Proksch, E., W. M. Holleran, G. K. Menon, P. M. Elias, and K. R. Feingold. 1993. Barrier function regulates epidermal lipid and DNA synthesis. *Br. J. Dermatol.* **128**: 473–482.
- Lampe, M. A., M. L. Williams, and P. M. Elias. 1983. Human epidermal lipids: characterization and modulations during differentiation. *J. Lipid Res.* **24**: 131–140.
- Lampe, M. A., A. L. Burlingame, J. Whitney, M. L. Williams, B. E. Brown, E. Roitman, and P. M. Elias. 1983. Human stratum corneum lipids: characterization and regional variations. *J. Lipid Res.* **24**: 120–130.

40. Ganesh Bhat, B., P. Wang, J. H. Kim, T. M. Black, T. M. Lewin, F. T. Fiedorek, Jr., and R. A. Coleman. 1999. Rat sn-glycerol-3-phosphate acyltransferase: molecular cloning and characterization of the cDNA and expressed protein. *Biochim. Biophys. Acta.* **1439**: 415–423.
41. Paulauskis, J. D., and H. S. Sul. 1988. Cloning and expression of mouse fatty acid synthase and other specific mRNAs. Developmental and hormonal regulation in 3T3-L1 cells. *J. Biol. Chem.* **263**: 7049–7054.
42. Li, Y., M. I. Gonzalez, J. L. Meinkoth, J. Field, M. G. Kazanietz, and G. I. Tennekoon. 2003. Lysophosphatidic acid promotes survival and differentiation of rat Schwann cells. *J. Biol. Chem.* **278**: 9585–9591.
43. Vance, J. E., and D. E. Vance. 2004. Phospholipid biosynthesis in mammalian cells. *Biochem. Cell Biol.* **82**: 113–128.
44. Vance, J. E., and D. E. Vance. 2005. Metabolic insights into phospholipid function using gene-targeted mice. *J. Biol. Chem.* **280**: 10877–10880.
45. Garg, A. 2004. Acquired and inherited lipodystrophies. *N. Engl. J. Med.* **350**: 1220–1234.
46. Coon, M., A. Ball, J. Pound, S. Ap, D. Hollenback, T. White, J. Tullinsky, L. Bonham, D. K. Morrison, R. Finney, et al. 2003. Inhibition of lysophosphatidic acid acyltransferase beta disrupts proliferative and survival signals in normal cells and induces apoptosis of tumor cells. *Mol. Cancer Ther.* **2**: 1067–1078.
47. Abraham, E., S. Bursten, R. Shenkar, J. Allbee, R. Tuder, P. Woodson, D. M. Guidot, G. Rice, J. W. Singer, and J. E. Repine. 1995. Phosphatidic acid signaling mediates lung cytokine expression and lung inflammatory injury after hemorrhage in mice. *J. Exp. Med.* **181**: 569–575.